IBRACON Structures and Materials Journal
Revista IBRACON de Estruturas e Materiais

ORIGINAL ARTICLE

Global second order effects in reinforced concrete buildings: simplified criterion based on Galerkin's method

Efeitos globais de segunda ordem em estruturas de concreto armado: critério simplificado com base no método de Galerkin

Rafael Nunes da Cunha[a] [ID]
Camila de Sousa Vieira[b] [ID]
Rainara Souza Gomes[b] [ID]
Ludmila dos Santos da Silva[b] [ID]
Ludmilson Abritta Mendes[b] [ID]
David Leonardo Nascimento de Figueiredo Amorim[a,b] [ID]

[a]Universidade Federal de Alagoas – UFAL, Programa de Pós-graduação em Engenharia Civil, Maceió, AL, Brasil
[b]Universidade Federal de Sergipe – UFS, Laboratório de Modelagem Matemática em Engenharia Civil, São Cristóvão, SE, Brasil

Abstract: Global second order effects in reinforced concrete buildings can be estimated using numerical or simplified methods, such as the γ_z coefficient, presented in the Brazilian standard. This paper proposes a new simplified parameter, which is deduced by the Galerkin's Method by Weighted Residuals. In order to evaluate the accuracy of the proposed methodology, 42 planar frames (21 framed system structures and 21 dual system structures) were analysed in terms of internal forces and displacements. Such results were compared to those obtained by the γ_z coefficient and to the reference results obtained throughout a geometric nonlinear elastic finite element program. The precision of the results was defined by statistical analyses, which showed that the results using the proposed parameter were closer to the reference ones, even in the recommended range for using the γ_z coefficient.

Keywords: global second order effects, reinforced concrete structures, weighted residuals, Galerkin's method.

Resumo: Efeitos globais de segunda ordem em edifícios de concreto armado podem ser estimados por métodos numéricos ou procedimentos simplificados, como o coeficiente γ_z, apresentado na norma brasileira. Neste artigo propõe-se um novo parâmetro simplificado, que é deduzido pelo Método de Galerkin por Resíduos Ponderados. De modo a avaliar a acurácia do modelo proposto, 42 pórticos planos (21 com contraventamento por pórticos e 21 com contraventamento por elementos rígidos) foram analisados em termos de esforços internos e deslocamentos. Tais resultados foram comparados aos obtidos pelo coeficiente γ_z e a resultados de referência obtidos por um programa de elementos finitos com análises de não linearidade geométrica. A precisão dos resultados foi definida por parâmetros estatísticos, que mostram que os resultados obtidos utilizando o parâmetro proposto estavam mais próximos dos resultados de referência, mesmo na faixa recomendada para a utilização do parâmetro γ_z.

Palavras-chave: efeitos globais de segunda ordem, estruturas de concreto armado, resíduos ponderados, Método de Galerkin.

1 INTRODUCTION

The design of tall buildings must take into account several factors, such as structure dimensions, wind velocity, terrain, nearby buildings and others ones that may increase lateral loads. Moreover, according to Khanduri et al. [1], for small buildings that have tall buildings nearby, the pressure gradient may induce a downward draft of air, which may cause high velocities and pressures.

International codes present ways to determine equivalent static lateral loads and suggest their application for building design [2]–[5]. These loads may be used to estimate lateral displacements, interstorey drift ratio and internal forces [6]–[8]; these variables can also be evaluated with computational methods [9].

The effects of lateral loads are very important to the design of buildings. Those loads increases the horizontal displacements and, therefore, the internal forces. Franco and Vasconcelos [10] discussed the criteria that structures may be classified as sway or non-sway, according to the increase of bending moments due to horizontal displacements. These displacements also must be considered correctly due to serviceability limit analysis and to an economic point of view. According to Algan [11], the relative displacement between storeys is also an important variable to be evaluated, because if interstorey ratio reaches the order of 0.5%, the repair cost may reach approximately half the price for the construction of new elements (partitions).

The increase of internal forces and displacements is called global second order effects. These effects must be considered in the structural design in order to evaluate the structural elements under maximum internal forces and to verify the displacements conditions.

There are several ways to consider the influence of global second order effects. NBR 6118 [12] suggests nonlinear or simplified procedures to estimate those effects, as the P-Delta method or α instability parameter, respectively. The latter option verify the necessity of consider the global second order effects. Beck and König [13] proposed the α instability parameter from the solution of an ordinary differential equation, using Bessel's functions. Other way to estimate those effects is to utilise amplification factors, which take into account the increase of the internal forces due to second order effects [12], [13]. NBR 6118 [12] suggests the use of the γ_z parameter, which was proposed by Franco and Vasconcelos [10]. That parameter was deduced using an incremental-iterative process, so it is a simplified method, and allows the estimation of global second order effects using only a first order analysis. This method is recommended only for the range $1.10 < \gamma_z \leq 1.30$ and achieves a good approximation for the global second order effects [14], [15].

Researches on sway analysis often propose improvements of existing parameters e.g., Ellwanger [16] that adjusted the α instability parameter and Souza et al. [17] that adjusted the γ_z coefficient by an amplification factor. Other ones propose new simplified parameters, such as Tekeli et al. [18], Cunha et al. [19] and Andrade and Nóbrega [20]. Several researchers study the α instability parameter, the γ_z coefficient as well as stability in general [21]–[36].

Therefore, the objective of this paper is to verify the quality of the criterion proposed by Cunha et al. [19] when analysing displacements of framed structures systems and internal forces of framed systems (resistance against lateral forces is formed only by beams and columns) and dual system structures (resistance against lateral forces is formed mostly by shear-walls). Note that the work presented by Cunha et al. [19] was published as an advance in the theme, but the results are limited to dual system structures and only assesses the horizontal displacement of the buildings. Now, the proposed formulation, which was developed with Galerkin's method by weighted residuals, is applied to 21 framed system structures and 21 dual system structures on the software MASTAN2 [37] to analyse displacements and internal forces.

2 SIMPLIFIED SWAY ANALYSIS BY THE Γ$_z$ COEFFICIENT

The γ_z coefficient was proposed by Franco and Vasconcelos [10] and it is presented in the Brazilian standard code [12]. The application of this parameter allows a simplified sway analysis of reinforced concrete buildings, and the estimation of global second order effects of these structures. Note that this was an important advance in the field, since Franco and Vasconcelos [10] stated: "The designer needs a simple method to decide whether a particular structure should be considered 'sway', without performing a second order analysis". Despite the previous existence of the instability parameter α [13], the γ_z coefficient is a clear improvement since it is calculated using the whole structure and it can be applied to estimate the global second order effects.

Consider that a building is represented by a simple vertical bar, whose length is L, and subjected to vertical and transversal uniform loads, equal to p and q, respectively (Figure 1). Moreover, consider that the bar properties have constant values: Young's modulus E, cross section area S and inertia moment I.
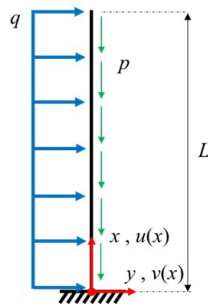
Figure 1. Vertical bar.

It is possible to define the first (M_1) and second order (M_2) bending moments at the clamped end of the vertical bar. Then, the γ_z parameter definition is:

$$\gamma_z = \frac{M_2}{M_1} \tag{1}$$

The second order bending moment may be calculated by the application of an incremental-iterative procedure, with n steps:

$$M_2 = M_1 + \Delta M_1 + \Delta M_2 + \Delta M_3 + \cdots + \Delta M_n \tag{2}$$

where ΔM is the increment of bending moments at each step of the incremental-iterative procedure.

Franco and Vasconcelos [10] admit that the increment rate of the bending moments $(r < 1)$ is constant until convergence, which is achieved by a geometric progression, which n is a high number i.e. $n \to \infty$:

$$r = \frac{\Delta M_1}{M_1} = \frac{\Delta M_2}{\Delta M_1} = \frac{\Delta M_3}{\Delta M_2} = \cdots = \frac{\Delta M_n}{\Delta M_{n-1}} < 1 \tag{3}$$

Equation 2 may be rewritten by applying Equation 3:

$$M_2 = M_1 + \Delta M_1 + \Delta M_2 + \Delta M_3 + \cdots + \Delta M_n = M_1 + rM_1 + r^2 M_1 + r^3 M_1 + \cdots + r^n M_1 = (1 + r + r^2 + r^3 + \cdots + r^n)M_1 \tag{4}$$

Equation 4 may be mathematically rearranged by multiplying it by $(1 - r)$:

$$(1 - r)M_2 = (1 - r^{n+1})M_1 \tag{5}$$

The convergence is only obtained with many steps i.e., $n \to \infty \Rightarrow r^{n+1} \to 0$, therefore Equation 5 may be simplified:

$$M_2 = \frac{1}{(1-r)}M_1 \tag{6}$$

The γ_z coefficient can be defined by substituting Equations 6 and 3 in (1), as shown in Equation 7:

$$\gamma_z = \frac{1}{1 - \frac{\Delta M_1}{M_1}} \tag{7}$$

being ΔM_1 the first increment of the nonlinear analysis, that can be calculated by a linear or first order analysis.

According to CEB/FIP [38], if the second order bending moments are 10% higher than the first order bending moments, the structure can be defined as a sway building and global second order effects must be considered. The Brazilian Standard Code NBR 6118 [12] defines a criteria based on the γ_z parameter: if its value are lower than 1.10, global second order effects can be neglected; if $1.10 < \gamma_z \leq 1.30$, global second order effects must be considered in the analysis and may be calculated by a first order analysis, by multiplying the lateral loads by $0.95\,\gamma_z$; for γ_z values higher than 1.30, NBR 6118 [12] does not recommend this simplified analysis and the second order global effects must be considered by others procedures, as a nonlinear analysis.

3 GALERKIN'S METHOD BY WEIGHTED RESIDUALS

The weighted residuals are a set of methods that are applied to solve differential equations in their week form, using any function as potential solution. Each method differs from the others by the chosen weight function. The criterion proposed in this paper is based on the Galerkin's method, by weighted residuals, since is a method that provides good results with simple equations.

3.1 Strong form

Consider a structure represented by a vertical bar, whose length is L, submitted to vertical and transversal loads equal to p and q, respectively (Figure 1). Moreover, consider that the bar has constant properties: Young's modulus E, cross section area S and inertia moment I. Admitting that the axial stiffness (ES) of the bar is high, the axial field displacement can be described, according to Equation 8, as:

$$u(x) = -\frac{pL^2}{2ES}\left[\frac{2x}{L} - \left(\frac{x}{L}\right)^2\right] \tag{8}$$

According to Powell [39], the bending moment field along the bar ($M(x)$), considering second order effects, may be described by:

$$M(x) = -EI\frac{d^2v(x)}{dx^2} + ES\left[\frac{du(x)}{dx} + \frac{1}{2}\left(\frac{dv(x)}{dx}\right)^2\right]v(x) \tag{9}$$

where EI is the flexural stiffness of the bar and $v(x)$ is the horizontal displacement field.

The bending moment field are related to the transversal load: $d^2M/dx^2 = -q$. Therefore, Equation 9 may be rewritten as:

$$-EI\frac{d^4v(x)}{dx^4} + ESv(x)\left(\frac{d^2v(x)}{dx^2}\right)^2 + ESv(x)\frac{dv(x)}{dx}\frac{d^3v(x)}{dx^3} + 2p\frac{dv(x)}{dx} + 2ES\frac{dv(x)}{dx^2}\left(\frac{dv(x)}{dx}\right)^2 - pL\left(1 - \frac{x}{L^2}\right)\frac{d^2v(x)}{dx^2} +$$
$$\frac{1}{2}ES\frac{d^2v(x)}{dx^2}\left(\frac{dv(x)}{dx}\right)^2 = -q \tag{10}$$

Note that the differential equation depends only of $v(x)$ and its derivatives. With the purpose of avoiding an iterative incremental procedure, the terms that depends more than once on $v(x)$ and its derivatives, are eliminated of the equation:

$$-EI\frac{d^4v(x)}{dx^4} + 2p\frac{dv(x)}{dx} - pL\left(1 - \frac{x}{L^2}\right)\frac{d^2v(x)}{dx^2} = -q \tag{11}$$

The biggest advantage of that simplification is the viability for design procedures, as Equation 11 does not need an incremental procedure. However, as some of the terms were removed from the equation that governs the problem, the equation also lost accuracy. Therefore, there is need of a correction factor to adjust the solution and compensate for the removed terms. This procedure is presented in section 4.

3.2 Weak form

The week form of a problem may be written using its strong form. Thus, from Equation 11, it is possible to define the residual function $R(x)$ (Equation 12). By definition, the residual function must be minimized along the problem domain to obtain accurate results.

$$\int_0^H R(x)\omega(x)dx = 0 \ \forall \omega(x)$$

$$\therefore R(x) = q - EI\frac{d^4v(x)}{dx^4} + 2p\frac{dv(x)}{dx} - pL\left(1 - \frac{x}{L^2}\right)\frac{d^2v(x)}{dx^2} \tag{12}$$

being $\omega(x)$ the weight function that must be continuous and homogeneous in the essential boundary conditions and $v(x)$ must obey the boundary conditions of the problem.

The transversal displacement field may be approximated by any function. In this paper, consider that $v(x)$ may be written, in indicial notation, as:

$$v(x) = \alpha_i\phi_i(x) \ \{i = 1, ..., n\} \tag{13}$$

being α_i the constants to be determinate, $\phi_j(x)$ the adopted functions and n the number of terms adopted in the approximation.

It is possible to assume any functions for $\omega(x)$. The Galerkin's methods applied for weight residuals proposed that the weight function is defined as:

$$\omega(x) = \beta_j\phi_j(x) \ \{j = 1, ..., n\} \tag{14}$$

where β_j are the constants of the $\omega(x)$ function and $\phi_j(x)$ are the same functions adopted for $v(x)$.

Therefore, substituting Equations 13-14 in Equation 12, for any values of β_j, it is possible to define the following system of linear equations:

$$K^T\alpha = F$$

$$\therefore \begin{cases} K_{ij} = \int_0^L \left[EI\frac{\partial^4\phi_i(x)}{\partial x^4}\phi_j(x) + 2p\frac{\partial\phi_i(x)}{\partial x}\phi_j(x) - pL\left(1 - \frac{x}{L}\right)\frac{\partial^2\phi_i(x)}{\partial x^2}\phi_j(x)\right]dx \\ \qquad\qquad F_j = \int_0^L q\phi_j(x)dx \end{cases} \tag{15}$$

4 PROPOSED CRITERION

Cunha et al. [19] presented a criterion for dual system frames, inspired in the γ_z parameter, which was deduced by the ratio of the second order and first order bending moments (Equation 1). The proposed criterion continues the research initially developed by Cunha et al. [19], by using the same concepts, and for application on framed system structures, as presented in Equation 16:

$$\zeta_g = \kappa\frac{M_2}{M_1} \tag{16}$$

being ζ_g the proposed coefficient, M_1 is the first order moment for a vertical bar (Figure 1), equal to $qL^2/2$, M_2 is the second order moment and κ is a parameter used to compensate the eliminated terms of Equation 10.

The Equation 15 was solved, adopting a complete fourth degree polynomial function as a potential solution for the approximation of the horizontal displacement field ($v(x)$). Based on the $v(x)$ result and knowing that the bending

Rev. IBRACON Estrut. Mater., vol. 17, no. 6, e17603, 2024

5/19

moment field for the vertical bar (Figure 1) is defined by $M = -EI(d^2v(x))/(dx^2)$, it is possible to define the bending moment field along the vertical bar. Therefore, the second order bending moment at the base ($x = 0$) is presented in Equation 17.

$$M_2 = \frac{-108EIqL^2[-21L^9p^3+8215EIL^6p^2-638550(EI)^2L^3p+9147600(EI)^3]}{259L^{12}p^4-140352EIL^9p^3+18993312(EI)^2L^6p^2-632681280(EI)^3L^3p+1975881600(EI)^4} \tag{17}$$

The proposed criterion can be applied for any frame, where L is the height of the building, q and p are the sum of all horizontal and vertical loads, respectively, distributed along the height L and EI is the equivalent stiffness of the frame.

The ζ_g parameter is applied in a similar way to the γ_z, aiming to obtain the second order results (internal forces and displacements) in a simplified way. For practical applications, the first order lateral loads must be multiplied by ζ_g, then applying the new loads at the structure and solving a first order analysis to get the approximated second order results.

5 METHODOLOGY

The present paper measured the displacement and internal forces (normal force, shear force and bending moment) of 21 framed system structures and 21 dual system structures, with different values of the γ_z parameter. For the first group of frames it is also proposed an analytical equation for the κ, based on the displacement results, by using the software Past! [40], which is an education statistical software, that provides a wide range of tools and visualizations for data exploration and visualization. All the simulations were made on the software MASTAN2, which is an interactive structural analysis program that provides preprocessing, analysis, and postprocessing capabilities, similar to today's commercially available structural analysis software. The program's linear and nonlinear analysis routines are based on the theoretical and numerical formulations presented by McGuire et al. [37]. Thus, for the second order analysis, it was used a prediction-correction algorithm [37], which provides results with high accuracy. The physical nonlinearity of the reinforced concrete was considered in a simplified way, according to item 15.7.3 of NBR 6118 [12], that suggests a reduction of the stiffness of the beams and columns in 60% and 20%, respectively. The frames were modelled according two different models: Type 1 (Figure 2a and Figure 3a) and Type 2 (Figure 2b and Figure 3b), being h the height of each story, adopted equal to 3 m. The properties of all the frames, the γ_z values and the parameters for the proposed model are presented in Table 1 and Table 2, for dual system and framed system structures, respectively, and the elasticity modulus was equal to 24 GPa. The sections of the structural elements were defined in order to have a set of different values for the γ_z parameter, even $\gamma_z \geq 1.30$, and check the quality of the proposed model also for this condition.
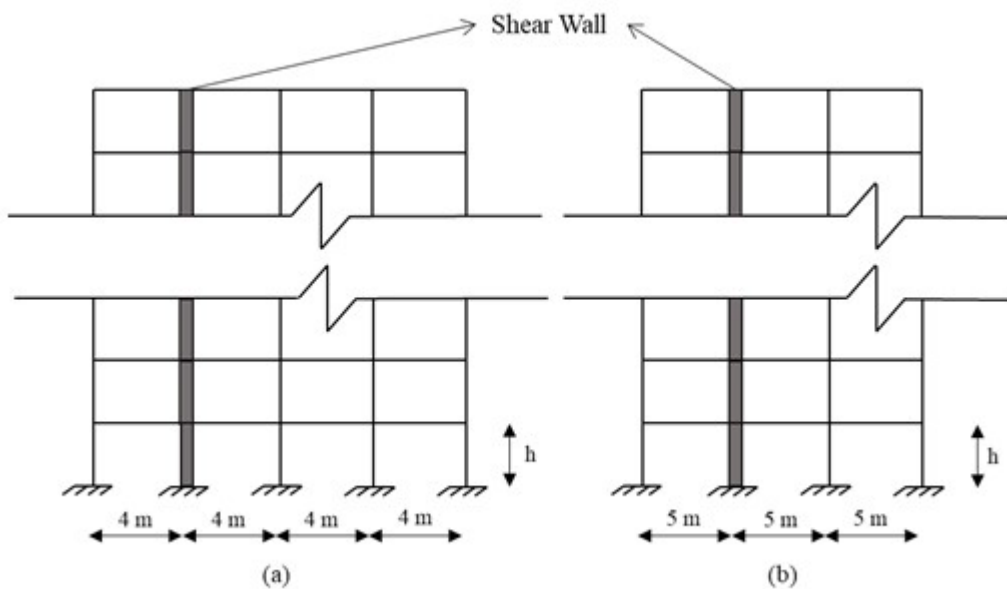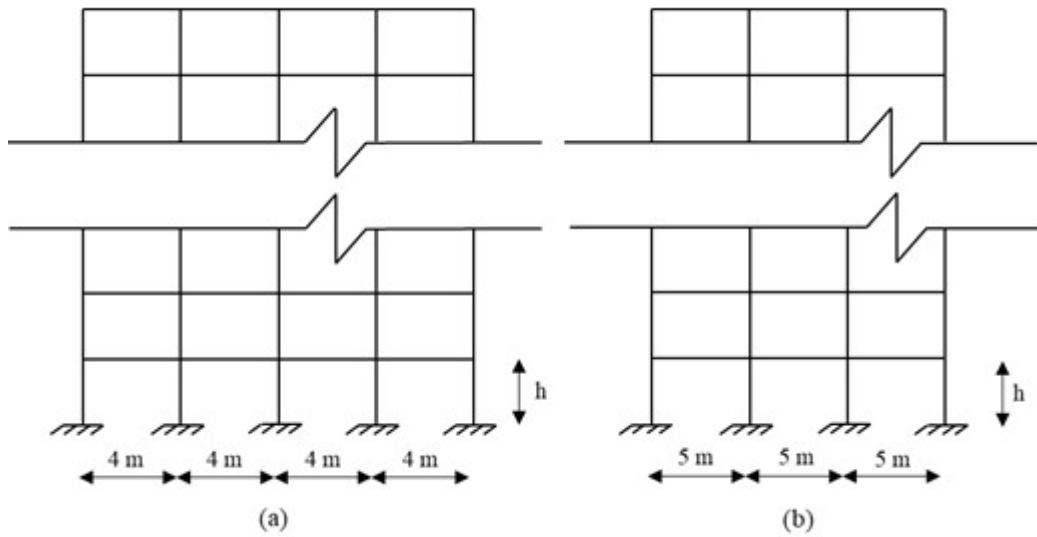

Figure 2. Frames models: dual system structures.

Rev. IBRACON Estrut. Mater., vol. 17, no. 6, e17603, 2024

6/19

Figure 3. Frames models: framed system structures.

Table 1. Dual system structures properties [19].

Frame	Type	Height	Cross-Section			γ_z	M_2/M_1	κ_o
			Beam	Column	Shear-Wall			
1	2	48	0.20×0.60	0.20×0.50	4.00×0.20	1.1150	1.48	0.78
2	1	24	0.15×0.40	0.25×0.30	1.50×0.25	1.1871	1.67	0.73
3	1	30	0.15×0.40	0.25×0.30	1.50×0.25	1.3225	2.67	0.53
4	2	54	0.20×0.60	0.20×0.50	4.00×0.20	1.1515	1.71	0.69
5	2	51	0.20×0.60	0.20×0.50	4.00×0.20	1.1325	1.58	0.72
6	1	36	0.15×0.40	0.25×0.30	2.00×0.25	1.2934	2.49	0.55
7	1	42	0.15×0.40	0.25×0.30	2.00×0.25	1.4587	6.46	0.24
8	2	66	0.20×0.60	0.20×0.50	4.00×0.20	1.2360	1.96	0.65
9	2	75	0.20×0.60	0.20×0.50	4.00×0.20	1.3287	2.81	0.50
10	2	81	0.20×0.60	0.20×0.50	4.00×0.20	1.4063	4.20	0.36
11	2	78	0.20×0.60	0.20×0.50	4.00×0.20	1.3656	3.34	0.43
12	2	84	0.20×0.60	0.20×0.50	4.00×0.20	1.4513	5.75	0.27
13	1	39	0.15×0.40	0.25×0.30	2.00×0.25	1.3626	3.40	0.43
14	2	69	0.20×0.60	0.20×0.50	4.00×0.20	1.2642	2.16	0.59
15	2	78	0.20×0.60	0.20×0.50	4.00×0.25	1.3344	2.96	0.48
16	2	81	0.20×0.60	0.20×0.50	4.00×0.25	1.3716	3.58	0.41
17	2	84	0.20×0.60	0.20×0.50	4.00×0.25	1.4127	4.62	0.33
18	2	81	0.20×0.60	0.20×0.50	4.00×0.29	1.3493	3.26	0.44
19	2	84	0.20×0.60	0.20×0.50	4.00×0.30	1.3823	3.95	0.37
20	2	87	0.20×0.60	0.20×0.50	4.00×0.30	1.4242	5.26	0.29
21	2	78	0.20×0.60	0.20×0.50	4.00×0.23	1.3459	3.10	0.46

Rev. IBRACON Estrut. Mater., vol. 17, no. 6, e17603, 2024

7/19

Table 2. Framed system structures properties.

| Frame | Type | Height | Cross-Section | | γ_z | M_2/M_1 | κ_o |
			Beam	Column			
1	2	48	0.20×0.60	0.20×0.50	1.1690	1.537	0.77
2	1	24	0.15×0.40	0.25×0.30	1.3767	2.128	0.68
3	1	30	0.15×0.40	0.25×0.30	1.5432	3.185	0.52
4	1	36	0.15×0.40	0.25×0.45	1.4735	2.757	0.57
5	2	51	0.20×0.60	0.20×0.50	1.1850	1.615	0.74
6	1	39	0.15×0.40	0.25×0.45	1.5496	3.617	0.46
7	1	42	0.15×0.40	0.25×0.45	1.6440	4.458	0.40
8	2	57	0.20×0.60	0.20×0.50	1.2201	1.815	0.69
9	1	27	0.15×0.40	0.25×0.30	1.4526	2.547	0.61
10	1	33	0.15×0.40	0.25×0.30	1.6575	4.132	0.44
11	2	45	0.20×0.60	0.20×0.50	1.1562	1.445	0.81
12	2	60	0.20×0.60	0.20×0.50	1.2481	1.640	0.77
13	2	63	0.20×0.60	0.20×0.45	1.3169	1.922	0.7
14	2	69	0.20×0.60	0.20×0.45	1.3738	2.252	0.63
15	2	69	0.20×0.60	0.20×0.40	1.4704	2.935	0.53
16	1	33	0.15×0.40	0.20×0.35	1.5836	3.376	0.5
17	1	36	0.15×0.40	0.20×0.35	1.6849	4.661	0.4
18	1	36	0.15×0.40	0.25×0.35	1.6226	3.838	0.46
19	1	39	0.15×0.40	0.20×0.60	1.4640	2.712	0.57
20	1	39	0.15×0.40	0.20×1.00	1.2887	1.949	0.68
21	2	60	0.20×0.60	0.20×0.55	1.2196	1.545	0.8

The proposed procedure is applicable for any type of lateral loads, as wind or the equivalent static load for earthquakes. In this paper, wind loads were adopted accordingly to the Brazilian Standard Code NBR 6123 [2], considering basic velocity (V_0) of 40 m/s, topography with slightly uneven terrain, on an urbanized area, with many residential or hotel buildings, which coefficients are shown in Equation 18:

$$S_1 = 1.0$$

$$S_2 = \begin{cases} 0.6374z^{0.125}, \text{if L} < 50\text{m} \\ 0.6156z^{0.135}, \text{if L} \geq 50\text{m} \end{cases}$$

$$S_3 = 1.0 \tag{18}$$

where z is the height of the analysed story.

For the sake of simplicity, the wind load calculated using the NBR 6123 [2] is given in Appendix A.

The vertical loads were determined accordingly NBR 6120 [41] for the occupation of offices and considering dead and live loads. The self-weight of the structural elements was also included in the analysis.

For the framed system structures, the simulations were performed with the aim to determine the best value of κ, in order to guarantee that the horizontal displacements obtained by the proposed procedure were closer to the reference ones, which were obtained with MASTAN2 by running a second order elastic analysis. All presented results were compared between the proposed procedure, the γ_z procedure and the MASTAN2 methods, being the latter adopted as reference.

The displacement results were analysed in a qualitative (displacement field behaviour) and quantitative (statistic methods) way. The results of maximum displacement, maximum positive bending moment, maximum negative bending moment and maximum shear force (for the beams) and maximum bending moment (for the columns) were compared by using statistical tests. It was applied the percent bias ($PBIAS$), the mean absolute error (MAE) and the mean absolute percentage error ($MAPE$) tests (Equation 19-21) for a global characterization of samples.

$$PBIAS = \frac{\sum_{i=1}^{n}(y_i - \hat{y}_1)}{\sum_{i=1}^{n} y_i} \qquad (19)$$

$$MAE = \frac{1}{n}\sum_{i=1}^{n}|y_i - \hat{y}_1| \qquad (20)$$

$$MAPE = \frac{1}{n}\sum_{i=1}^{n}\frac{|y_i - \hat{y}_1|}{y_i} \qquad (21)$$

where y_i is the reference value, $\hat{y}_1$ is the simulated value and n is the sample size.

It was also verified the hypothesis of the average values of the analysed results being from the same population. Before running this mean test, it was verified the hypothesis of normal distribution of the samples (i.e., the normality of the samples), by Shapiro-Wilk test. If the p-values were higher than the level of significance, the homoscedasticity test (which tests the hypothesis of the samples have the same finite variance) were performed using the Bartlett's test, otherwise, it was used the Levene's test. If the p-values of both tests did not allow rejecting the null hypothesis, the t-test were performed to verify if the samples are from the same population. Otherwise, it was performed the Mann-Whitney test (for a detailed review of the statistical tests see [42]). For all tests, it was adopted a level of significance of 5%.

Cunha et al. [19] evaluated previously the dual system structures in terms of displacements. The present paper also compared the values of internal forces for this structural system, similar to the framed system structures, added the maximum bending moment at the shear-wall. Also, it was performed the same statistical tests used for the framed system structures.

6 RESULTS AND DISCUSSIONS

6.1 Framed system structures

6.1.1 Nonlinear regression

Twenty-one framed system structures were solved by a first order analysis with the goal of define an equation that describes the behaviour of the κ coefficient, according to the value of M_2/M_1. It was chosen the best value of κ that leads to the closest fit of the Horizontal displacement vs. Storey of the frames to the reference results (MASTAN2 results). These Horizontal displacement vs. Storey curves are presented for all frames in Figure 4, with the values of κ and a direct comparison with the first order analysis, γ_z analysis and MASTAN2. The values of κ and M_2/M_1 are also presented in Table 1 and Table 2, for the dual system and framed structures, respectively. Based in the values for all framed structures (Table 2), it was performed a nonlinear regression, using the software Past! [40], which results is the Equation 22:

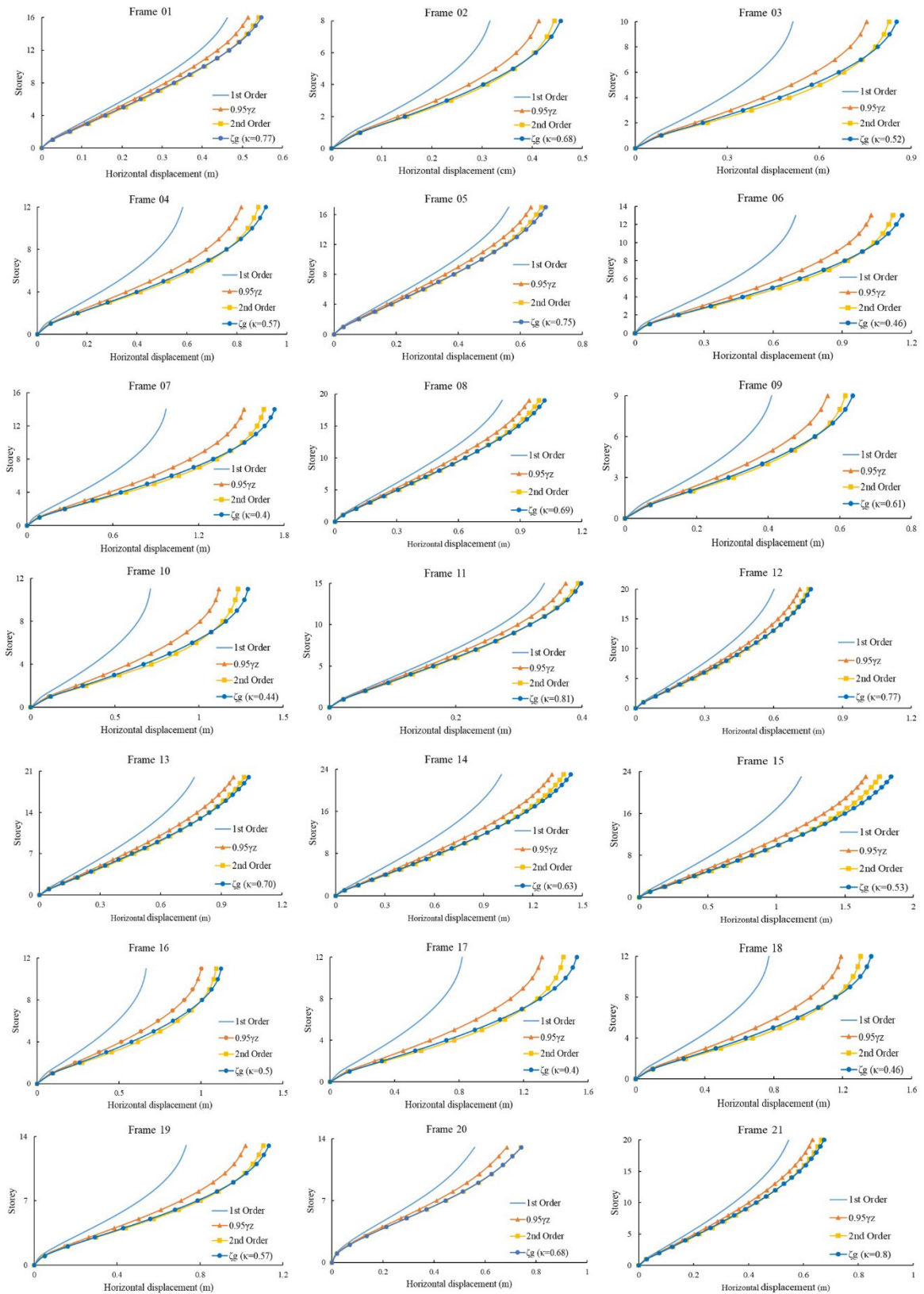$$\kappa_{Framed} = -0.95743 + 1.9154\left(\frac{M_2}{M_1}\right)^{-0.22608} \qquad (22)$$

Rev. IBRACON Estrut. Mater., vol. 17, no. 6, e17603, 2024

9/19

Figure 4. Horizontal displacements results.

Rev. IBRACON Estrut. Mater., vol. 17, no. 6, e17603, 2024

10/19

The behaviour observed in proposed equation is quite similar to the one previously presented by Cunha et al. [19] for dual system structures (Equation 23).

$$\kappa_{Dual} = -0.3864 + 1.3644 \left(\frac{M_2}{M_1}\right)^{-0.4205} \tag{23}$$

To verify the quality of the adjust that Equation 22 provides, it was made the Nash-Sutcliffe coefficient [43], according to the Equation 24:

$$NSE = 1 - \frac{\sum_{t=1}^n (\kappa_p^t - \kappa_o^t)^2}{\sum_{t=1}^n (\kappa_o^t - \kappa_o^{Avg})^2} \tag{24}$$

where κ_p^t is the predicted coefficient by Equation 22, κ_o^t is the observed coefficient and κ_o^{Avg} is the average of the observed coefficients. The Nash-Sutcliffe coefficient determines the magnitude of the residual variance in relation to the observed data variance, which values are in the range $-\infty < NSE \leq 1$. The unitary value means a perfect fit of the points to the model; $NSE = 0$ means that the values obtained by Equation 22 are as precise as the mean of the observed data; and $NSE < 0$ indicates that the mean of the observed data provides a better prediction than the Equation 22 [43]. For the proposed model, the NSE efficiency coefficient was equal to 0.9901.

Many assumptions are made when a regression analysis is performed, as the normality of the errors (i.e., the sample follows a normal distribution) and that the random variables are uncorrelated [42]. To check the normality hypothesis, the Shapiro-Wilk test was used on the residuals from the regression. The p-value for this test was equal to 0.65, higher than the level of significance. Therefore, it is not possible to reject the hypothesis that the sample follow a normal distribution and corroborate that the proposed model did not present inconsistences.

6.1.2 Displacement analysis

The Horizontal displacement vs. Storey curves of the structures (Figure 4) provide an initial supposition that the results obtained by the proposed criterion leads to better results along all structure, than the γ_z ones, compared to the MASTAN2. One way to verify this hypothesis is performing a series of statistical analysis. As the NBR 6118 [12] indicates that the γ_z parameter only is recommended for the range $1.10 < \gamma_z \leq 1.30$, the analysis were made for two samples: all frames and the frames whose value of γ_z are in the recommended range. The basic statistics parameters and the *PBIAS*, *MAE* and *MAPE* results are presented in Table 3.

Table 3. Basic statistics of displacements.

	All frames			$1.10 < \gamma_z \leq 1.30$		
	γ_z	ζ_g	MASTAN2	γ_z	ζ_g	MASTAN2
Mean (m)	0.913	1.016	0.984	0.643	0.689	0.679
Standard deviation (m)	0.353	0.408	0.384	0.176	0.192	0.186
PBIAS (%)	-7.726	3.191	-	-5.704	1.463	-
MAE (m)	0.071	0.032	-	0.037	0.010	-
MAPE (%)	7.493	2.799	-	5.680	1.387	-

The results presented in Table 3 shows that the γ_z model leads to values of displacement lower than the reference ones, while the proposed model, higher and closer displacements for the two samples analysed. The PBIAS parameter also indicates that the ζ_g model presents lowers absolute bias. The MAE e MAPE parameters indicate that the results of the proposed model are in favour of security and with errors lower than the γ_z model, in comparison to the second order results. The mean tests were also performed for the two samples, which results are presented in Table 4. Based on the p-values, it is not possible to reject the hypothesis of normal distribution of the models (normality). Moreover, it was also verified the hypothesis of homoscedasticity, which p-value increases for the range $1.10 < \gamma_z \leq 1.30$.

The results of the t-test did not allow the rejection of the hypothesis that both models have means statistical equals to the reference values. Although, there is greater certainty in affirm that proposed model is more similar to the reference values, as shown by the p-values results. Therefore, it is possible to conclude that the proposed model leads to better results and in favour of security, in terms of displacement. This analysis is important to better conclusions for the serviceability limits analysis or interstorey drift ratio that may cause high increase in the repair costs [11].

Table 4. p-values of the statistical tests of displacements.

	All frames			$1.10 < \gamma_z \leq 1.30$		
	Normality	Homoscedasticity	Mean test	Normality	Homoscedasticity	Mean test
MASTAN2	0.7032		-	0.8476		-
γ_z	0.6920	0.8134	0.5389	0.8261	0.9792	0.7118
ζ_g	0.6426		0.7922	0.8119		0.9222

6.1.2 Internal forces analysis

In a sway analysis is also important to analyze the results in terms of internal forces. Then, the same tests made for the displacement were made for beams: positive bending moment, negative bending moment and shear force (Table 5 and Table 6) and for the columns: bending moments (Table 7 and Table 8).

Table 5. Basic statistics of internal forces for the beams.

		All frames			$1.10 < \gamma_z \leq 1.30$		
		γ_z	ζ_g	MASTAN2	γ_z	ζ_g	MASTAN2
Positive bending moments	Mean (kNm)	346.957	391.210	420.686	371.514	402.443	422.000
	Standard deviation (kNm)	171.925	187.554	191.702	134.868	147.031	157.716
	PBIAS (%)	-21.250	-7.535	-	-13.589	-4.860	-
	MAE (kNm)	73.729	29.600	-	50.486	19.929	-
	MAPE (%)	18.161	7.454	-	11.464	4.294	-
Negative bending moments	Mean (kNm)	-558.924	-604.748	-641.229	-589.743	-622.229	-653.500
	Standard deviation (kNm)	176.326	190.243	198.959	142.792	153.055	162.840
	PBIAS (%)	-14.726	-6.032	-	-10.811	-5.026	-
	MAE (kNm)	82.305	36.481	-	63.757	31.271	-
	MAPE (%)	-12.765	-5.652	-	-9.445	-4.521	-
Shear forces	Mean (kN)	336.957	356.690	370.257	374.314	389.600	399.643
	Standard deviation (kN)	99.926	106.168	109.858	79.871	85.037	89.500
	PBIAS (%)	-9.883	-3.803	-	-6.767	-2.578	-
	MAE (kN)	33.300	13.567	-	25.329	10.043	-
	MAPE (%)	8.911	3.642	-	6.099	2.366	-

Table 6. p-values of the statistical tests of internal forces for the beams.

		All frames			$1.10 < \gamma_z \leq 1.30$		
		Normality	Homoscedasticity	Mean test	Normality	Homoscedasticity	Mean test
Positive bending moments	MASTAN2	0.4929		-	0.8157		-
	γ_z	0.2294	0.8805	0.1970	0.8077	0.9341	0.5319
	ζ_g	0.2686		0.6173	0.8600		0.8144
Negative bending moments	MASTAN2	0.7066		-	0.3461		-
	γ_z	0.5465	0.8657	0.1637	0.7491	0.9531	0.4511
	ζ_g	0.5631		0.5471	0.8146		0.7177
Shear forces	MASTAN2	0.3809		-	0.4611		-
	γ_z	0.2537	0.9146	0.3103	0.3867	0.9645	0.5867
	ζ_g	0.1434		0.6862	0.4641		0.8332

The basic statistical parameters (Table 5) provide an initial idea about the behaviour of the internal forces. It is possible to note that, for all analysis, the results obtained by the proposed model (ζ_g) are closer to the reference ones (MASTAN2) than the γ_z model, even in the range recommended by the NBR 6118 [12]. This conclusion can be reached by the mean and standard deviation or by the PBIAS, MAE and MAPE parameters, which errors with the γ_z model are, at least, twice the values of the proposed parameter. Moreover, it is not possible to reject the hypothesis of normal distribution and homoscedasticity of the models, for the two samples analysed, and it was possible to apply t test (Table 6). The p-values did not allow to reject the hypothesis of both simplified models are equal to the reference one. However, as observed for the displacement results, the p-values for the proposed model are higher than the γ_z model and, therefore, there is a lower chance of committing an error in this affirmation.

Table 7. Basic statistics of bending moments for the columns.

	All frames			1.10 < γ_z ≤ 1.30		
	γ_z	ζ_g	MASTAN2	γ_z	ζ_g	MASTAN2
Mean (kNm)	648.105	715.810	651.852	714.771	766.500	718.900
Standard deviation (kNm)	276.276	302.021	277.736	377.730	412.326	386.295
PBIAS (%)	-0.578	8.935	-	-0.578	6.210	-
MAE (kNm)	9.576	63.957	-	17.014	47.600	-
MAPE (%)	1.782	9.830	-	2.979	6.785	-

Table 8. p-values of the statistical tests of bending moments for the columns.

	All frames			1.10 < γ_z ≤ 1.30		
	Normality	Homoscedasticity	Mean test	Normality	Homoscedasticity	Mean test
MASTAN2	0.0084		-	0.0059		-
γ_z	0.0106	0.9511	0.8999	0.0056	0.9942	0.7983
ζ_g	0.0160		0.3924	0.0055		0.6093

The results for the bending moments in the columns of the framed structures indicates that the proposed model presents higher errors than the γ_z model, in comparison to the reference ones (Table 7). However, it is possible to note that the errors of the proposed model are positive i.e., the bending moments are in favour of the security, while the ones by the γ_z model are lowers (negative PBIAS). It is important to note that, for the range of 1.10 < γ_z ≤ 1.30, the results obtained by the proposed model got an improvement, while the ones achieved by the γ_z model worsened. The same conclusion can be reached by the analysis of the mean tests (Table 8).

6.2 Dual system structures: internal forces analysis

Cunha et al. [19] previously studied dual system structures focusing on the displacement of the structures. These authors concluded that the results in terms of displacement of the proposed model was better than the ones by the γ_z model, similar to the conclusions reached for the framed system structures (section 6.1). This paper focuses on the analysis of the internal forces of the beams: positive bending moment, negative bending moment and shear force (Table 9 and Table 10) and of the columns: bending moments (Table 11 and Table 12) and of the shear-walls (Table 13 and Table 14).

Table 9. Basic statistics of internal forces for the beams.

		All frames			$1.10 < \gamma_z \leq 1.30$		
		γ_z	ζ_g	MASTAN2	γ_z	ζ_g	MASTAN2
Positive bending moments	Mean (kNm)	624.443	671.376	675.586	722.986	777.829	784.086
	Standard deviation (kNm)	325.409	357.521	360.394	264.453	296.758	300.973
	PBIAS (%)	-8.190	-0.627	-	-4.261	0.230	-
	MAE (kNm)	51.143	6.419	-	16.943	5.671	-
	MAPE (%)	6.735	1.122	-	4.107	1.440	-
Negative bending moments	Mean (kNm)	-510.548	-552.362	-552.129	-561.014	-605.871	-604.171
	Standard deviation (kNm)	153.271	173.281	171.044	130.558	154.080	151.865
	PBIAS (%)	-8.144	0.042	-	-5.211	-0.293	-
	MAE (kNm)	41.581	5.919	-	20.586	2.414	-
	MAPE (%)	-7.214	-0.999	-	-5.012	-0.657	-
Shear forces	Mean (kN)	336.167	355.490	355.310	369.357	390.471	389.629
	Standard deviation (kN)	86.734	96.241	95.223	61.981	73.026	71.925
	PBIAS (%)	-5.694	0.051	-	-3.375	-0.183	-
	MAE (kN)	19.143	2.771	-	9.471	1.071	-
	MAPE (%)	5.096	0.719	-	3.241	0.404	-

Table 10. p-values of the statistical tests of internal forces for the beams.

		All frames			$1.10 < \gamma_z \leq 1.30$		
		Normality	Homoscedasticity	Mean test	Normality	Homoscedasticity	Mean test
Positive bending moments	MASTAN2	0.0127		-	0.2628		-
	γ_z	0.0110	0.8679	0.3924	0.3457	0.9914	0.8770
	ζ_g	0.0124		0.8405	0.3257		0.9932
Negative bending moments	MASTAN2	0.1858		-	0.3583		-
	γ_z	0.1873	0.8410	0.4117	0.3234	0.9924	0.7469
	ζ_g	0.2498		0.9965	0.3315		0.9851
Shear forces	MASTAN2	0.0475		-	0.1229		-
	γ_z	0.0345	0.8889	0.2683	0.1049	0.9946	0.8080
	ζ_g	0.0655		0.9599	0.1147		0.9894

Similar to the observed in the framed structures, the results obtained for the beams, applying the proposed model, are closer to the reference ones, in comparison to the ones achieved by the γ_z model. In terms of errors (Table 9), the internal forces obtained by the proposed model are, at least, almost three times lower than the ones by the γ_z model, even in the recommended range of this parameter. The mean test also corroborates this analysis, which p-values are near to 1.0 (perfect correlation between the samples).

Table 11. Basic statistics of bending moments for the columns.

	All frames			$1.10 < \gamma_z \leq 1.30$		
	γ_z	ζ_g	MASTAN2	γ_z	ζ_g	MASTAN2
Mean (kNm)	486.852	523.933	526.638	533.157	576.557	581.957
Standard deviation (kNm)	220.585	241.850	247.061	205.253	230.338	235.291
PBIAS (%)	-8.172	-0.516	-	-4.973	-0.032	-
MAE (kNm)	40.024	6.438	-	14.914	2.814	-
MAPE (%)	6.751	1.460	-	4.674	0.880	-

Table 12. p-values of the statistical tests of bending moments for the columns.

	All frames			$1.10 < \gamma_z \leq 1.30$		
	Normality	Homoscedasticity	Mean test	Normality	Homoscedasticity	Mean test
MASTAN2	0.0085		-	0.7764		-
γ_z	0.0089	0.8306	0.3143	0.8326	0.9893	0.8185
ζ_g	0.0099		0.8209	0.8149		0.9988

The results for the columns are similar to that observed in the beams, which errors with the proposed parameter are quite lower than the γ_z model. The Brazilian normative parameter leads to internal forces lower than the reference values (PBIAS) and higher errors (MAE and MAPE) for all structures. For the recommended range of γ_z parameter, the results are better, although with higher errors, which may also be concluded by the p-values of the mean test. The p-value improved in the second sample (0.3143 to 0.8185), however lower than the value of the proposed parameter for all structures (0.8209), which achieved the value of 0.9988 for the range $1.10 < \gamma_z \leq 1.30$.

Table 13. Basic statistics of bending moments for the shear-wall.

	All frames			$1.10 < \gamma_z \leq 1.30$		
	γ_z	ζ_g	MASTAN2	γ_z	ζ_g	MASTAN2
Mean (kNm)	3.37E+04	3.75E+04	3.41E+04	3.83E+04	4.25E+04	3.89E+04
Standard deviation (kNm)	1.83E+04	2.07E+04	1.83E+04	1.54E+04	1.79E+04	1.53E+04
PBIAS (%)	-1.253	9.094	-	-2.850	4.439	-
MAE (kNm)	5.65E+02	3.41E+03	-	5.73E+02	9.60E+02	-
MAPE (%)	2.204	8.806	-	3.223	4.608	-

Table 14. p-values of the statistical tests of bending moments for the shear-wall.

	All frames			$1.10 < \gamma_z \leq 1.30$		
	Normality	Homoscedasticity	Mean test	Normality	Homoscedasticity	Mean test
MASTAN2	0.2215		-	0.3108		-
γ_z	0.2072	0.8118	0.9407	0.4249	0.9879	0.9213
ζ_g	0.2032		0.5744	0.4019		0.8725

The results for the shear-walls are similar to that observed in the columns of the framed system structures. The proposed parameter leads to higher errors than the γ_z model, however, with values above the reference ones, while the γ_z model, lower. Moreover, for the recommend range of the γ_z parameter, the results by this model worsened, while the proposed model improved for all evaluated parameters, also observed by the p-values of the mean tests.

7 CONCLUSIONS

The present paper proposed a simplified method to estimate the global second order effects in reinforced concrete structures, especially the framed system ones, and made a review of the method for dual system structures. The procedure was deduced using Galerkin's method by weighted residuals and has applicability similar to the γ_z parameter, proposed in the NBR 6118 [12].

Twenty-one 21 framed system structures were evaluated to define an analytical equation for the ζ_g parameter, whose quality was verified by the Nash-Sutcliffe coefficient [43] and obtained a quality of 0.9901, being 1.00 a perfect adjustment. The results of the structures using the proposed model and the γ_z model were compared to the reference values (MASTAN2) in terms of displacement and internal forces. The comparisons were made by using visual and statistical parameters (*PBIAS*, *MAE*, *MAPE*, normality, homoscedasticity, and mean test). Based on the analysed structures, the proposed model leads to responses closer to the reference values than the γ_z coefficient, even in the range

recommended by the NBR 6118 [12]. The results of *PBIAS*, *MAE* and *MAPE* for the proposed model reached values of, at least, half of the γ_z model. The normality of the samples was verified by using the Shapiro-Wilk Normality test and the Bartlet test for the homoscedasticity test, before applying the mean test. The results observed by the *PBIAS*, *MAE* and *MAPE* were corroborated by these tests, which p-values for the proposed model were higher than the ones for the γ_z model. Therefore, for the analysed examples, the proposed model is more similar to the reference values. This conclusion was made for displacement and internal forces in the beams. For the bending moments in the columns, the proposed model leads to results higher than the reference ones, in favour of security, which errors reduce when the analysed structures are in the $1.10 < \gamma_z \leq 1.30$ range, while the γ_z coefficient leads to worst results.

The same analyses were made for the dual system structures, in terms of internal forces. The conclusions were similar to those observed for the framed system structures, which errors were quite lower for the proposed model, than the γ_z model, and the p-values, in certain cases, reaching values near to 1.0. These conclusions concern all internal forces of beams columns. For the internal forces in the shear-wall, it was observed a behaviour similar to the columns in the framed system, which the proposed model leads to higher values of bending moments, that reduces when analysed in the $1.10 < \gamma_z \leq 1.30$ range, reaching to errors and p-values near to the γ_z model.

In sum, for the analysed examples, the proposed model is more accurate than the one that uses the γ_z coefficient. Moreover, the proposed model maintains its accuracy even when the γ_z coefficient range is violated in its upper limit ($\gamma_z \leq 1.30$). For future researches, it is recommended to verify the accuracy of the proposed model for three-dimensional structures. If these models were appropriately tested, it might be considered as another simplified method to assess the stability of buildings in a future update of the NBR 6118 [12].

ACKNOWLEDGEMENTS

REFERENCES

[1] A. C. Khanduri, T. Stathopoulos, and C. Bédard, "Wind-induced interference effects on buildings - a review of the state-of-the-art," *Eng. Struct.*, vol. 20, no. 7, pp. 617–630, 1998, http://dx.doi.org/10.1016/S0141-0296(97)00066-7.

[2] Associação Brasileira de Normas Técnicas, *Forças Devidas ao Vento em Edificações*, NBR 6123, 1988.

[3] Architectural Institute of Japan, "Wind loads," in *Recommendations for Loads on Buildings*. Tokyo, Japan: Architectural Inst. Jpn., 1993, ch. 6, pp. 42–47.

[4] B. Standard *Eurocode 1: Actions on structures*, United Kingdom: British Standard, 2006.

[5] American Society of Civil Engineers, *Minimum design loads and associated criteria for buildings and other structures*, American Society of Civil Engineers, 2017.

[6] H. S. Hu, R. T. Wang, Z. X. Guo, and B. M. Shahrooz, "A generalized method for estimating drifts and drift components of tall buildings under lateral loading," *Struct. Des. Tall Spec.*, vol. 29, no. 2, pp. e1688, 2020, http://dx.doi.org/10.1002/tal.1688.

[7] J. Y. Fu, Q. X. Zheng, J. R. Wu, and Y. Q. Huang, "Wind-induced inter-story drift analysis and equivalent static wind load for multiple targets of tall buildings," *Struct. Des. Tall Spec.*, vol. 25, no. 6, pp. 297–321, 2016, http://dx.doi.org/10.1002/tal.1259.

[8] American Concrete Institute (ACI) Committee, "*Building code requirements for structural concrete (ACI 318-19) and commentary*", 2019.

[9] A. D. M. Wahrhaftig and M. A. D. Silva, "Using computational fluid dynamics to improve the drag coefficient estimates for tall buildings under wind loading," *Struct. Des. Tall Spec.*, vol. 27, no. 3, pp. 1–12, 2018, http://dx.doi.org/10.1002/tal.1442.

[10] M. Franco and A. C. Vasconcelos, "Practical assessment of second order effects in tall buildings", in *Colloq. CEB-FIP MC90*, Rio de Janeiro, RJ, Brazil, 1991, pp. 307-324.

[11] B. B. Algan, "Drift and damage Consideration in earthquake resistance design of reinforced concrete buildings," PhD Thesis, Univ. Illinois, Illinois, 1982.

[12] Associação Brasileira de Normas Técnicas, *Projeto de Estruturas de Concreto – Procedimento*, NBR 6118, 2023.

[13] H. Beck and G. König, "Restraining forces in the analysis of tall buildings" in *Symp. On Tall Buildings*, Pergamon Press, Oxford, 1966, pp. 513-536. https://doi.org/10.1016/B978-0-08-011692-1.50029-8.

[14] J. R. Bueno and D. D. Loriggio, "Analysis of second order effects: case study," *Rev. IBRACON Estrut. Mater.*, vol. 9, no. 4, pp. 494–509, 2016, http://dx.doi.org/10.1590/S1983-41952016000400002.

[15] F. C. Freitas, L. A. R. Luchi, and W. G. Ferreira, "Global stability analysis of structures and actions to control their effects," *Rev. IBRACON Estrut. Mater.*, vol. 9, no. 2, pp. 192–213, 2016, http://dx.doi.org/10.1590/S1983-41952016000200003.

[16] R. J. Ellwanger, "A variable limit for the instability parameter of wall-frame or core-frame bracing structures," *Rev. IBRACON Estrut. Mater.*, vol. 5, no. 1, pp. 104–136, 2019, http://dx.doi.org/10.1590/S1983-41952012000100008.

[17] T. P. Souza, R. G. S. Lima, R. N. Cunha, L. A. Mendes, and D. L. N. D. F. Amorim, "Amplification factor for simplified sway estimate by the γ_z coefficient," *J. Braz. Soc. Mech. Sci.*, vol. 44, no. 12, pp. 582, 2022, http://dx.doi.org/10.1007/s40430-022-03891-3.

[18] H. Tekeli, E. Atimtay, and M. Turkmen, "A simplified method for determining sway in reinforced concrete dual buildings and design applications," *Struct. Des. Tall Spec.*, vol. 22, no. 15, pp. 1156–1172, 2013, http://dx.doi.org/10.1002/tal.761.

[19] R. N. Cunha, L. A. Mendes, and D. L. N. D. F. Amorim, "Proposal of a simplified criterion to estimate second order global effects in reinforced concrete buildings," *Rev. IBRACON Estrut. Mater.*, vol. 13, no. 2, pp. 200–211, 2020, http://dx.doi.org/10.1590/S1983-41952020000200002.

[20] R. B. Andrade and P. G. B. D. Nóbrega, "Second-order torsion effects in concrete buildings", *Rev. IBRACON Estrut. Mater.*, vol. 14, no. 1, pp. e14105, 2020. https://doi.org/10.1590/S1983-41952021000100005.

[21] K. A. Zalka, "A hand method for predicting the stability of regular buildings, using frequency measurements," *Struct. Des. Tall Spec.*, vol. 12, no. 4, pp. 273–281, 2003, http://dx.doi.org/10.1002/tal.221.

[22] L. A. B. Cicolin and J. R. Figueiredo Fo., "Stability of reinforced concrete buildings with flat slabs: influence of frames with flat slab layers and inverted edge beams," *Rev. IBRACON Estrut. Mater.*, vol. 4, no. 3, pp. 501–529, 2011, http://dx.doi.org/10.1590/S1983-41952011000300008.

[23] D. M. Oliveira, N. A. Silva, C. F. Bremer, and H. Inoue, "Considerações sobre a determinação do coeficiente γ_z," *Rev. IBRACON Estrut. Mater.*, vol. 6, pp. 75–100, 2013, http://dx.doi.org/0.1590/S1983-41952013000100005.

[24] M. M. S. Lacerda, A. C. Florêncio, W. A. D. Silva, and R. G. Delalibera, "Avaliação dos critérios para análise da estabilidade global em edifícios de concreto armado: estudo de caso", *Rev. Eletronica Eng. Civ.*, vol. 9, no. 2, pp. 24–37, 2014, http://dx.doi.org/10.5216/reec.v9i2.28875.

[25] L. A. Feitosa and E. C. Alves, "Study of global stability of tall buildings with prestressed slabs," *Rev. IBRACON Estrut. Mater.*, vol. 8, pp. 196–224, 2015, http://dx.doi.org/10.1590/S1983-41952015000200008.

[26] V. M. Passos, L. A. Feitosa, E. C. Alves, and M. S. Azevedo, "Analysis of instability of tall buildings with prestressed and waffle slabs," *Rev. IBRACON Estrut. Mater.*, vol. 9, pp. 244–262, 2016, http://dx.doi.org/10.1590/S1983-41952016000200006.

[27] J. Y. Fu, Q. X. Zheng, J. R. Wu, and Y. Q. Huang, "Wind-induced inter-story drift analysis and equivalent static wind load for multiple targets of tall buildings," *Struct. Des. Tall Spec.*, vol. 25, no. 6, pp. 297–321, 2016, http://dx.doi.org/10.1002/tal.1259.

[28] E. C. Alves and J. F. M. Paixão, "Análise de estabilidade global em edifícios altos" *Rev. Eletronica Eng. Civ.*, vol. 13, no. 1, pp. 48–63, 2017, http://dx.doi.org/10.5216/reec.v13i1.39552.

[29] F. F. Leitão, G. H. Siqueira, L. C. M. Vieira Jr., and S. J. C. Almeida, "Analysis of the global second-order effects on irregular reinforced concrete structures using the natural period of vibration," *Rev. IBRACON Estrut. Mater.*, vol. 12, pp. 408–428, 2019, http://dx.doi.org/10.1590/S1983-41952019000200012.

[30] C. W. S. Diniz, E. N. Lages, and A. S. R. Barboza, "Global stability of buildings' structural systems considering beam-wall connections," *Rev. IBRACON Estrut. Mater.*, vol. 12, pp. 705–737, 2019, http://dx.doi.org/10.1590/S1983-41952019000400002.

[31] E. C. Alves and L. A. Feitosa, "Analysis of the global tall buildings stability in flat slabs considering the soil structure interaction," *Rev. IBRACON Estrut. Mater.*, vol. 13, pp. 183–199, 2020, http://dx.doi.org/10.1590/S1983-41952020000100013.

[32] H. S. Hu, R. T. Wang, Z. X. Guo, and B. M. Shahrooz, "A generalized method for estimating drifts and drift components of tall buildings under lateral loading," *Struct. Des. Tall Spec.*, vol. 29, no. 2, pp. e1688, 2020, http://dx.doi.org/10.1002/tal.1688.

[33] L. D. B. Lecchi, W. G. Ferreira, P. M. M. P. P. Costa, and A. M. C. Sarmanho, "Comparison between exact and approximate methods for geometrically nonlinear analysis prescribed in design standards for steel and reinforced concrete structures," *Rev. IBRACON Estrut. Mater.*, vol. 15, no. 1, pp. e15101, 2021. https://doi.org/10.1590/S1983-41952022000100001.

[34] M. G. Aboelhassan, M. E. Shoukry, and S. M. Allam, "Effect of the connecting beam stiffness on the bracing limit for reinforced concrete slender columns in single and multi-story frames," *Rev. IBRACON Estrut. Mater.*, vol. 15, no. 2, pp. , e15209, 2021. https://doi.org/10.1590/S1983-41952022000200009.

[35] T. P. Santos and A. S. R. Barboza, "Estabilidade global em edifício alto de concreto considerando a modelagem e o posicionamento do núcleo rígido," *Rev. IBRACON Estrut. Mater.*, vol. 101, pp. 54–60, 2021, http://dx.doi.org/10.4322/1809-7197.2021.101.0005.

[36] O. C. Marques, L. A. Feitosa, K. V. Bicalho, and E. C. Alves, "Analysis of constructive effect and soil-structure interaction in tall building projects with shallow foundations on sandy soils," *Rev. IBRACON Estrut. Mater.*, vol. 14, pp. e14103, 2020, http://dx.doi.org/10.1590/S1983-41952021000100003.

[37] W. McGuire, R. H. Gallagher, and R. D. Ziemian, *Matrix Structural Analysis*, 2nd ed., Lewisburg: Bucknell University, 2014.

[38] Comité Euro-Internacional Du Béton, *Final Draft* (Bulletin D'Information, 203/204/205). Lausanne, Switzerland: Comité Euro-Internacional Du Béton, 1991.

[39] G. H. Powell, "Theory of nonlinear elastic structures," *J. Struct. Div.*, vol. ST12, pp. 2687–2701, 1969.

[40] Ø. Hammer, D. A. T. Harper, and P. D. Ryan, "Past: paleontological statistics software package for educaton and data anlysis," *Palaeontol. Electronica*, vol. 4, no. 1, pp. 1-9, 2001.

[41] Associação Brasileira de Normas Técnicas, *Ações para o Cálculo de Estruturas de Edificações*, NBR 6120, 2019.

[42] D. C. Montgomery and G. C. Runger, *Applied Statistics and Probability for Engineers,* Hoboken, Nova Jersey, EUA: John Wiley & Sons, 2007.

[43] J. E. Nash and J. V. Sutcliffe, "River flow forecasting through conceptual models part I – A discussion of principles," *J. Hydrol. (Amst.)*, vol. 10, pp. 282–290, 1970.

Rev. IBRACON Estrut. Mater., vol. 17, no. 6, e17603, 2024

18/19

APPENDIX A – WIND LOADS

The wind loads were calculated according to the NBR 6123 [2] recommendations, which are presented in Tables A1 and A2, for structures lower and higher than 50 m, respectively. If the storey is the last one of the structures, the wind load should be half of the presented value due to the wind influence area.

Table A1. Wind loads for structures lower than 50 m.

Storey	Load (kN)	Storey	Load (kN)
1	36.00	9	65.15
2	43.41	10	67.03
3	48.43	11	68.78
4	52.34	12	70.42
5	55.59	13	71.95
6	58.40	14	73.41
7	60.88	15	74.79
8	63.11	16	76.10

Table A2. Wind loads for structures higher than 50 m.

Storey	Load (kN)	Storey	Load (kN)	Storey	Load (kN)	Storey	Load (kN)
1	35.40	9	61.31	17	71.88	25	79.16
2	42.10	10	62.95	18	72.92	26	79.94
3	46.59	11	64.47	19	73.91	27	80.69
4	50.06	12	65.89	20	74.86	28	81.43
5	52.94	13	67.22	21	75.78	29	82.15
6	55.40	14	68.48	22	76.67		
7	57.58	15	69.67	23	77.52		
8	59.54	16	70.80	24	78.35		

Rev. IBRACON Estrut. Mater., vol. 17, no. 6, e17603, 2024

19/19